

Supporting Information

A novel aptasensor based endogenous enzyme-powered DNA walker for ATP imaging in specific living cells

Chunrong Li,^a Tong Li,^b Mingqi Guo,^b Tiehong Meng,^a Jing Peng,^b Simin Liu,^b Qianyu Wang,^{a,*} Baoping Xie,^{b,*} Zong Dai,^c Jun Chen^{b,*}

^a Qiannan Medical College for Nationalities, Duyun, 558000, China.

^b NMPA Key Laboratory for Research and Evaluation of Drug Metabolism, Guangdong Provincial Key Laboratory of New Drug Screening, School of Pharmaceutical Sciences, Southern Medical University, Guangzhou, 510515, China.

^c Key Laboratory of Sensing Technology and Biomedical Instrument of Guangdong Province, School of Biomedical Engineering, Sun Yat-Sen University, Shenzhen 518107, China.

E-mail: 327854055@qq.com, xiebp@smu.edu.cn, chenj258@smu.edu.cn

Experimental Procedures

Materials and reagents. All DNA sequences were procured from Sangon Biotech Co., Ltd. (Shanghai, China) and subsequently purified using high-performance liquid chromatography (HPLC). The sequences of the oligonucleotides are provided in Table S1. Other reagents including adenosine triphosphate (ATP), guanosine triphosphate (GTP), uridine triphosphate (UTP), cytidine triphosphate (CTP), diethyl pyrocarbonate (DEPC)-treated water, 40% acrylamide, 4S GelRed nucleic acid stain, and β -mercaptoethanol were also sourced from Sangon Biotech Co., Ltd. For the preparation of double-stranded WA, strands W and A were incubated at 95°C for five minutes, followed by a controlled cooling process to achieve annealing at 18°C for 50 min, and then stored at 4°C until further use. Apurinic/aprimidinic endonuclease 1 (APE1) was acquired from New England Biolabs (Beijing, China). Additionally, antibiotics penicillin and streptomycin, Dulbecco's Modified Eagle Medium (DMEM), trypsin, fetal bovine serum (FBS), and phosphate buffered saline (PBS, pH 7.4) were obtained from Beyotime Biotechnology Co., Ltd. (Shanghai, China). Throughout the experimental procedures, DEPC-treated water was used to maintain RNase-free conditions.

Gel electrophoresis was performed using a DyCZ-24DN cell (LIUYI, Beijing, China) and DigiGenius gel system (Syngene, UK). Agarose gel was pictured by FlourChem R (USA). Transmission electron microscopy (TEM) images of the prepared samples were obtained using a JEM 1011 electron microscope (Japan). Dynamic light scattering (DLS) and zeta potential analyses of the prepared samples were conducted using a Malvern Nano-ZS particle sizer and zeta potential analyzer (UK). Fluorescence emission spectra were acquired with a WATERS Prep 150 fluorescence spectrophotometer (WATERS, USA). Ultraviolet-visible absorption spectra were recorded using a Hitachi U-2910 UV-Vis spectrophotometer (Japan). Cell laser scanning confocal microscopy (CLSM) images were captured with a FV3000 confocal scanning system (Olympus Corporation, Japan), utilizing a 63x oil-immersion objective lens. MTT assay results were documented using a M1000PRO Multifunctional Microplate Reader (TECAN, Austria). Flow cytometric analysis was performed on Sysmex CyFlow Cube 8 (Japan).

Preparation of AuNPs. Initially, the glassware required for the reaction was sterilized by immersion in aqua regia and thoroughly rinsed with deionized water to prepare for the synthesis. Subsequently, under boiling conditions, 5 mL of a 38.8 mM trisodium citrate solution was rapidly added to a two-necked round-bottom flask containing 17

mL of a 0.1% (w/v) gold(III) chloride (HAuCl_4) solution and 33 mL of deionized water. The reaction solution turned deep red within one minute, indicating the formation of AuNPs. The mixture was then heated for an additional 20 minutes under reflux conditions before the heat source was turned off. While maintaining stirring, the reaction system was allowed to cool slowly to room temperature, ultimately yielding AuNPs with a diameter of 13 nm.

Fluorescence Assay. A series of ATP concentrations (0.01 mM, 0.1 mM, 0.5 mM, 1 mM, 3 mM, 5 mM, 7.5 mM) were added to a mixture containing 1 nM DNA walker, 5 U/ml APE1, 50 mM Tris-HCl, and 20 mM MgCl_2 . After incubation at 37°C for 2 hours, the fluorescence intensity of the samples was measured using a fluorescence spectrophotometer. The fluorescence spectra from 545 nm to 630 nm were recorded with an excitation wavelength of 515 nm, and the fluorescence intensity at 553 nm was used as the readout signal.

ATP Imaging in living Cells. Cells were seeded in a 20 mm confocal dish to achieve 80-85% confluence. After washing three times with PBS, 500 μL of Opti-MEM containing 0.4 nM DNA walker was added to the dish and incubated for a period of time. Following staining with Hoechst for 15 minutes, cells were observed using FV3000 with laser excitation at 405 nm for Hoechst and 514 nm for Cy3.

To optimize imaging time, 0.4 nM of DNA walker was added to multiple confocal dishes and incubated for different durations (0, 0.5, 1, 1.5, and 2 hours). Cells were washed three times with PBS and imaged using CLSM.

In the investigation of ATP level fluctuation, three groups of MCF-7 cells were treated differently. The first group was treated with oligomycin (10 μM) for 30 min to inhibit ATP expression and reduce its level. The second group served as the control. The third group was treated with an ATP enhancer of CaCl_2 (5.0 mM) for 30 min to increase ATP expression levels. Subsequently, all three groups of HeLa cells were incubated with 0.4 nM of DNA walker. Finally, cells were washed three times with PBS and imaged using CLSM.

DNA Walker Preparation. To synthesize the DNA walker, the butanol dehydration method was employed to modify the thiol-modified strand S and WA onto AuNPs via Au-S bonds. For complete hybridization of W and A, they were mixed in a 1:1.5 ratio in PBS buffer. The mixture was then incubated at 95°C for 5 minutes before the temperature was adjusted to 18°C for an additional 50 minutes to obtain WA, which was stored at 4°C until further use. Before modification on the gold nanoparticles, S

and WA were each incubated with TCEP (0.4 mM) at 37°C for one hour to reduce disulfide bonds. In the presence of NaCl (7.5 mM), the solutions of S and WA were added to AuNPs in a final volume of 100 uL, followed by the immediate addition of 900 uL of n-butanol and rapid vortexing for several seconds. Then, 100 uL of 0.5×TBE was added, followed by a second round of vortex mixing. The resulting solution was rapidly centrifuged to separate the liquid phase; with the DNA nanomachine DNA walker solution present in the lower layer. To collect the DNA walker, the lower layer was centrifuged at 15000g for 20 minutes, washed with 10 mM Tris-HCl, and centrifuged three times. Finally, the obtained DNA walker was stored at 4°C until further use.

Electrophoresis Analysis. The reaction of WA and S in solution was verified using polyacrylamide gel electrophoresis. Mixtures containing different combinations of DNA strands were incubated at 37 °C for 60 min. An 8% polyacrylamide gel was prepared using 1 × TBE buffer (89 mM triboric acid, 2 mM EDTA). Appropriate amounts of the DNA strand mixtures after reaction were loaded into different lanes of the polyacrylamide gel. Electrophoresis was carried out in 0.5×TBE at a constant voltage of 200 V for 45 minutes. The gel was then stained with 4S GelRed stain for 15 minutes and imaged using the DigiGenius gel imaging system (Syngene, UK) for analysis. To further verify the feasibility of the DNA walker, mixtures containing different combinations of functionalized gold nanoparticles were incubated at 37 °C for 60 min. An agarose gel was prepared by adding 0.6 g of agarose to 30 mL of 0.5×TBE electrophoresis buffer. Appropriate amounts of the reaction solutions were carefully mixed with glycerol and loaded into the gel wells. After electrophoresis at 90 V for 1 hour, the gel was observed using an ultraviolet transilluminator and the bands were recorded using a FlourChem R gel imaging system.

Cell Incubation. MCF-7, MCF-10A, and MDA-MB-231 cells were all obtained from the Shanghai Institute of Life Sciences and cultured in DMEM medium supplemented with 10% FBS and 1% antibiotics. The cells were incubated in a humidified atmosphere at 37°C with 5% CO₂.

Flow cytometry assay. MCF-7 cells were cultured into 6-well plates for 24 h with 2 mL DMEM medium. The cells were transfected with different type of DNA walkers for 1.5 h (the operation was the same as the confocal imaging), then cells were thoroughly washed two times in PBS buffer and detached by trypsin-EDTA. These treated cells

were centrifuged at 1000 rpm for 4 min and were re-suspended with 1.0 mL PBS for flow cytometric analysis on Sysmex CyFlow Cube 8 (Japan). Fluorescence was determined by counting 10000 usable events, and the data were analyzed by the FlowJo software.

Quantitation Assay for ATP. The ATP content was measured using a commercial ATP kit. Cells were seeded in 6 wells plates and cultured overnight at 37 °C for 24 h in a 5% CO₂ incubator. The cells were washed with PBS three times to remove the excess medium before added 200 µL of the cell lysate provided by the ATP kit. The cells were lysed completely in an ice bath environment and the homogenate was centrifuged at 12,000g for 5 min at 4°C to get the supernatant. The ATP content of cell lysates was measured with ATP assay kit (luminometer). The concentration of intracellular ATP was calculated by assuming an average volume of a cell was ~2000 µm³.

S1. Table S1.

Table S1 Sequences of the Used Oligos

| Name | Sequences (5'-3') |
|---|---|
| walk strand (W) | ATCATACCCCCAGGTGACTGTGTTTTTTTTTTTTTT TTTTTTTTTT-SH |
| Aptamer probe (A) | <i>CACAGTCACCTGGGGGAGTATTGCGGAGGAAGG</i> T |
| Substrate reporter probe (S) | Cy3-ACCTGGG <i>X</i> GTATGATGTTTTTTTTTT-SH |
| Substrate reporter probe without AP sites (Sn) | Cy3-ACCTGGGAGTATGATGTTTTTTTTTT-SH |
| Random Aptamer probe (A _R) | <i>CACAGTCACCTGGGGGAGTATTACAAACCAACC</i> T |

S2. The characterization of the Aptasensor.

13 nm AuNPs were obtained via the chloroauric acid reduction method. TEM was first used to characterize the morphology of the AuNPs and functionalized AuNPs. TEM images showed that functionalized AuNPs have greater dispersity compared to bare AuNPs (Figure S1A and S1B), consistent with previous reports. The Zeta potential also changed from -13.8 to -30.6 mV (Figure S1C). The dynamic light scatter measured an increase in the hydrodynamic diameter of the AuNPs from 18 nm to 58 nm after the modification with nucleic acid probes (Figure S1D). Notably, the average particle size determined by dynamic light scattering (DLS) exceeds that measured by transmission electron microscopy (TEM), as DLS yields the hydrodynamic diameter, whereas TEM provides the actual physical dimensions.

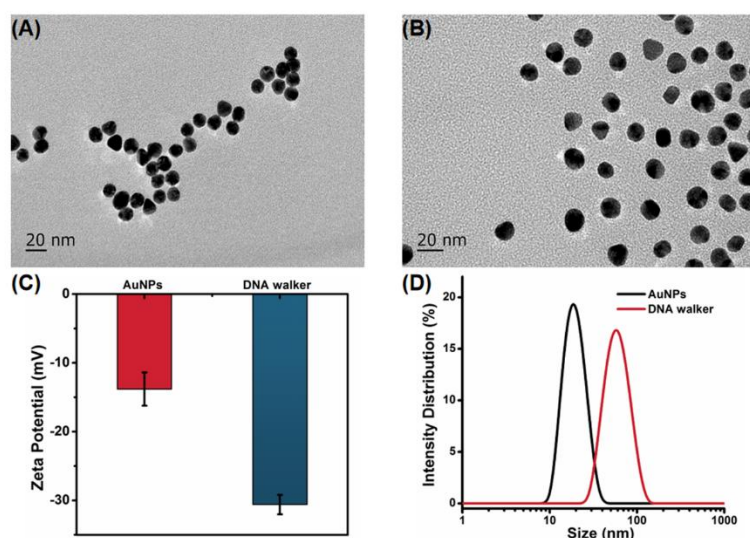


Figure S1. (A) TEM images of AuNPs, (B) TEM images of functionalized AuNPs, (C) Zeta potential of AuNPs (red column) and DNA walker (blue column) (D) Hydrate particle size of AuNPs before and after modification.

S2. UV-Vis adsorption spectra of AuNP and DNA walker.

Compared with bare AuNPs, the UV/Vis absorption spectrum of functionalized AuNPs also exhibited red shift (Figure S2). The above results indicate that the nucleic acid probes were successfully modified on the surface of the AuNPs.

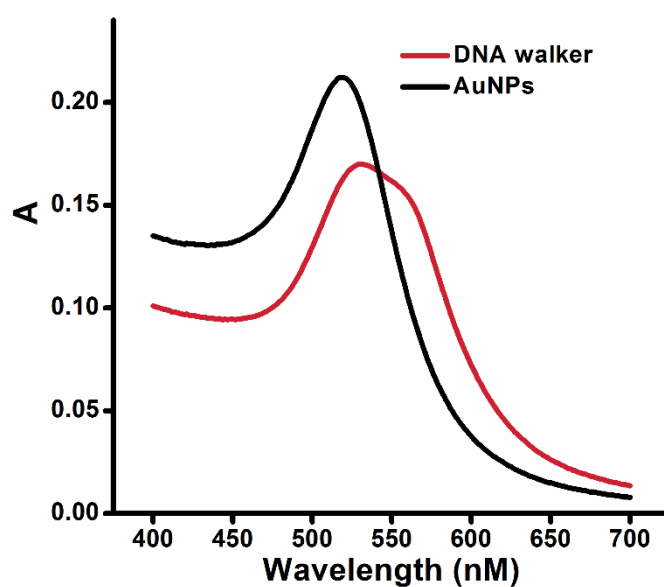


Figure S2. UV-Vis adsorption spectra of AuNP and DNA walker.

S3. PAGE analysis to characterize the ATP stimuli responsive behavior.

When WA was mixed with ATP, a distinct W band was observed (lane 5), indicating that ATP could successfully bind with the A of WA and release the W chain. When WA, S, and APE1 were mixed, substrate S and WA remained stable (lane 8). Only when WA, S, APE1, and ATP were incubated together, a distinct band with a lower molecular weight was observed (lane 7), which should be the product after the removal of the AP site of substrate S. These results indicate that the designed probes can operate as expected. After modifying WA and S onto the surface of AuNPs,

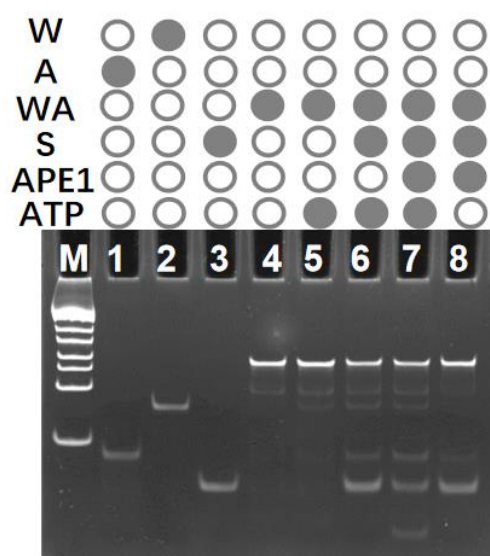


Figure S3. PAGE analysis to characterize the ATP stimuli responsive behavior. Lane 1: A, Lane 2: W, Lane 3: S, Lane 4: WA, Lane 5: WA and ATP; Lane 6: WA, S and ATP; Lane 7: WA, S and ATP in the presence of APE1; Lane 8: WA and S in the presence of APE1.

S4. Fluorescence response of DNA walker with AP site and nAP-DNA walker without AP site.

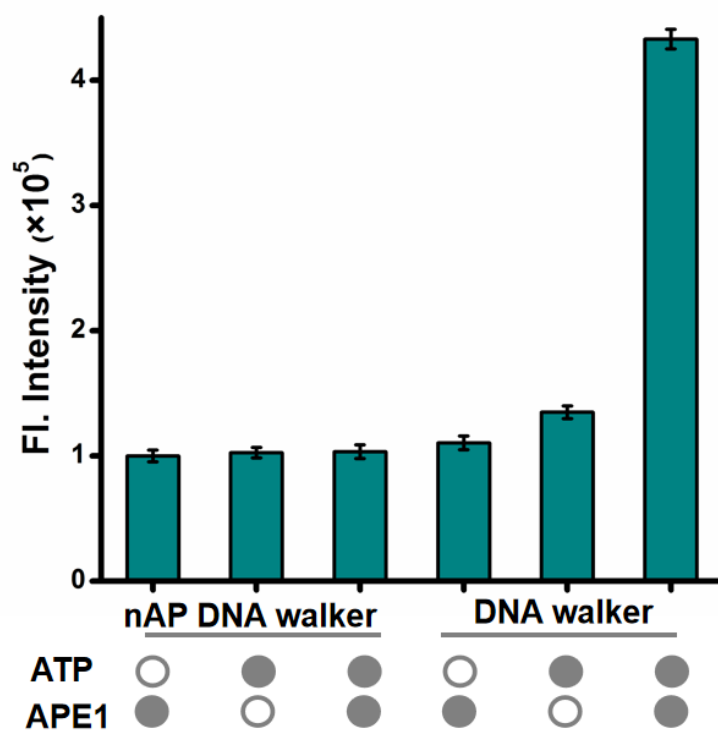


Figure S4. Specificity of the DNA walker. To verify the DNA nanomotors couldn't be activated without the addition of target ATP and APE1, two types of DNA nanomotors were designed including DNA walker and nAP-DNA walker, especially, there was no modification of the AP site in nAP-DNA walker. 0.5 mM ATP or 10 U/mL APE1 were added to the DNA walker and nAP-DNA walker.

S5. Optimization of the reaction conditions of DNA walker.

The ratio of WA to S chain was first optimized. Different ratios of WA and S were mixed and modified onto the surface of AuNPs. The signal-to-noise ratio F/F_0 was used to evaluate the response performance, where F and F_0 represent the fluorescence values measured with and without ATP, respectively. The maximum signal-to-noise ratio F/F_0 was obtained when the ratio of WA to S chain was 1:5. Therefore, we chose a ratio of W/A to S of 1:5 for subsequent experiments (Figure S5). Based on the ratio of W/A to S, the number of WA and S modified on each gold nanoparticle is approximately 14 and 70, respectively (Figure S6). We further monitored the real-time fluorescence curve of the sensor in the presence or absence of ATP. As shown in Figure S7, as the reaction time extended, the background fluorescence signal did not enhance significantly, while the fluorescence intensity of the group with ATP increased with incubation time and stabilized at about 60 minutes. Therefore, we chose 1 h as the optimal reaction time. We also studied the effect of different concentrations of APE1 on the performance of this aptasensor. The experimental results are shown in Figure S8, the fluorescence signal increased with the increase of APE1 concentration within 5 U/mL, and the fluorescence intensity gradually reached a plateau when the concentration of APE1 exceeded 5 U/mL. This indicates that a concentration of 5 U/mL APE1 is sufficient to drive the DNA walker. Therefore, we chose 5 U/mL as the optimal enzyme amount.

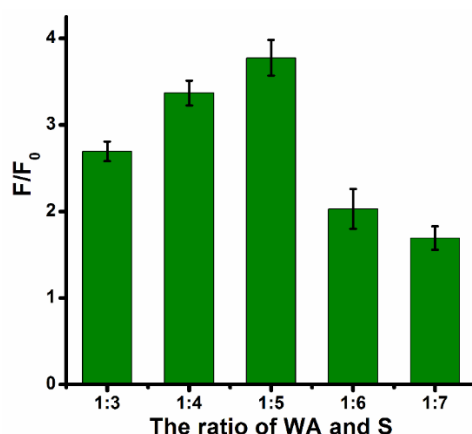


Figure S5. (A) Optimization of ratio of WA and S in the developed strategy. (n=3)

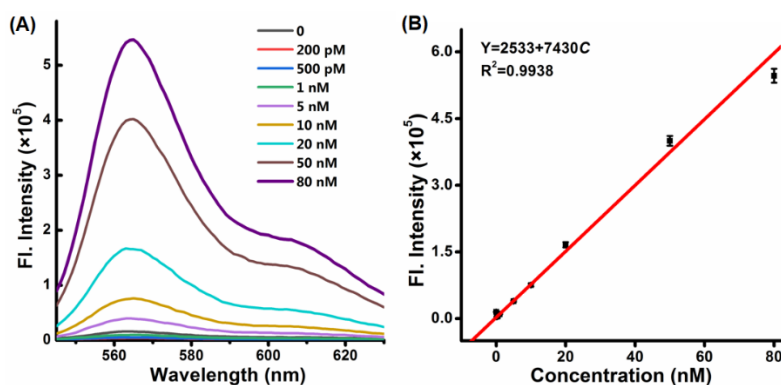


Figure S6. Calculate the number of substrates on AuNPs. A) fluorescence spectra in the presence of different concentrations of substrates; B) calibration curve between fluorescence intensity and different concentrations of substrates (n=3).

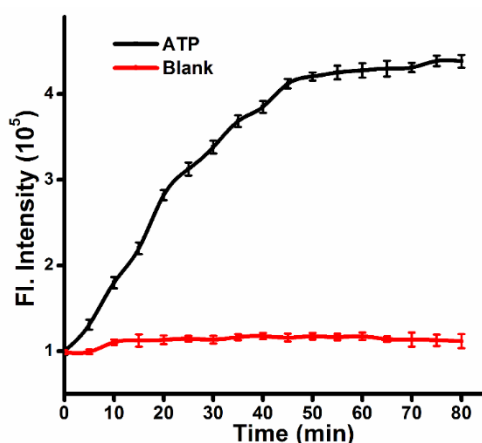


Figure S7. Real-time fluorescence curves of DNA walker in the presence or absence of ATP. Error bars show the standard deviations of three independent experiments.

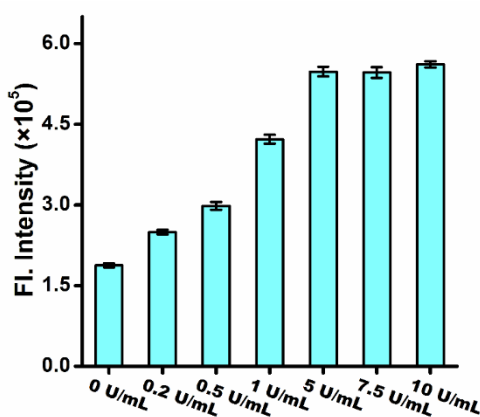


Figure S8. The effect of APE1 on the performance of DNA walker. 0 U/mL, 0.2 U/mL, 0.5 U/mL, 1 U/mL, 5U/mL, 7.5U/mL and 10 U/mL was added to the reaction solution respectively (n=3).

S5. Fluorescence spectra of the DNA walker probe in response to different concentrations of ATP.

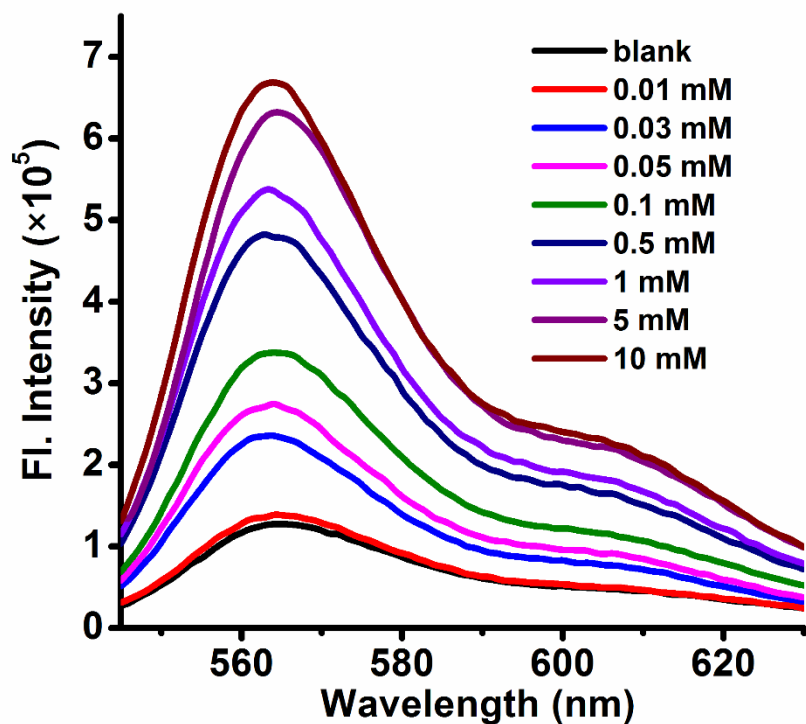


Figure S9. Fluorescence spectra of the DNA walker probe in response to different concentrations of ATP.

S6. Stability investigation of the DNA walker.

The resistance of nanoprobe to nuclease degradation is crucial for achieving imaging in complex biological systems. DNase I is a common endonuclease in cells, which can cleave phosphodiester bonds in the DNA backbone and degrade single / double stranded DNA molecules into small fragments. To detect the stability of the proposed system, we selected DNase I to study the degradation of DNA walker. When the DNA walker system was incubated with different concentrations of DNase I for 6 h, only slight changes of fluorescence intensity were observed (Figure S10), indicating that the developed aptasensor with high stability.

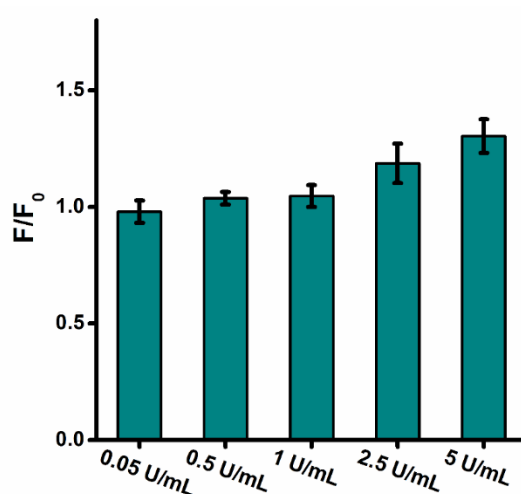


Figure S10. Stability investigation of the DNA walker with different concentrations of DNase I. 0 U/mL; 0.05 U/mL; 0.5 U/mL; 1 U/mL; 2.5 U/mL; 5 U/mL DNase I were added to the 0.4 nM DNA walker with 1×PBS solution respectively and incubated for 6 h; F and F₀ represent the fluorescence intensities of EEPDN in the presence and absence of the ATP. Error bars show the standard deviations of three independent experiments.

S7. Cytotoxicity of the DNA walker.

MTT assays were used to evaluate the cytotoxicity of the DNA walker. After incubation of the DNA walker system with MCF-7 cells for 24h, cell viability was above 90% when the concentrations of DNA walker within 0.6 nM (Figure S11), demonstrating good biocompatibility of the DNA walker system.

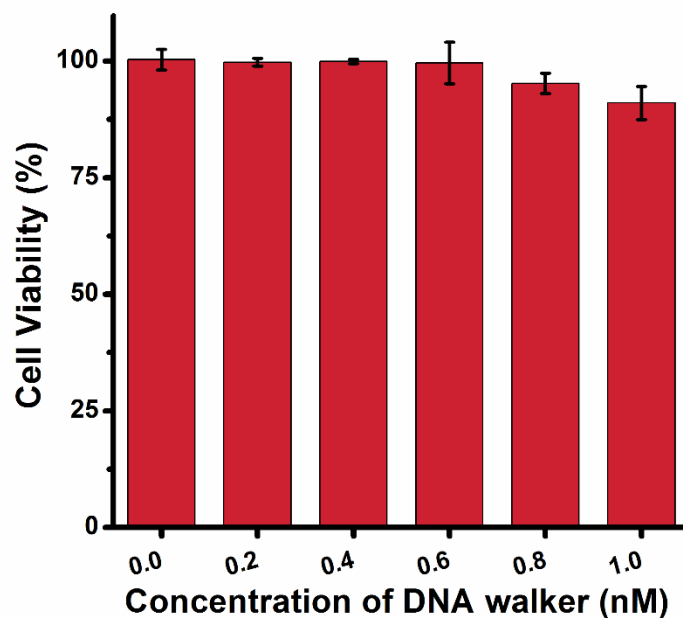


Figure S11. Normalized Cell viability of MCF-7 cells incubated with different concentrations of DNA walker probes for 24 h. Error bars show the standard deviations of three independent experiments.

S8. Flow cytometric analysis of the feasibility of the DNA walker.

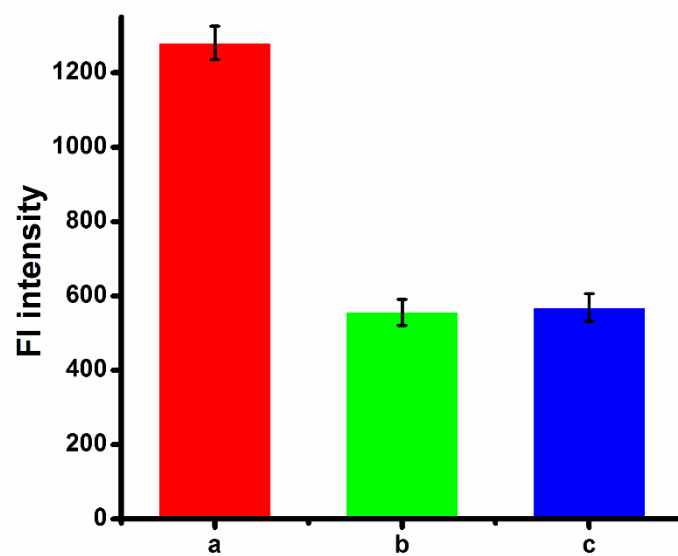


Figure S12. Flow cytometric quantification of fluorescence of HeLa cells treated with (a) DNA walker, (b) R-DNA walker, (c) nAP-DNA walker. Error bars show the standard deviations of three independent experiments.

S9. Impact of APE1 inhibitors on DNA walker for ATP imaging.

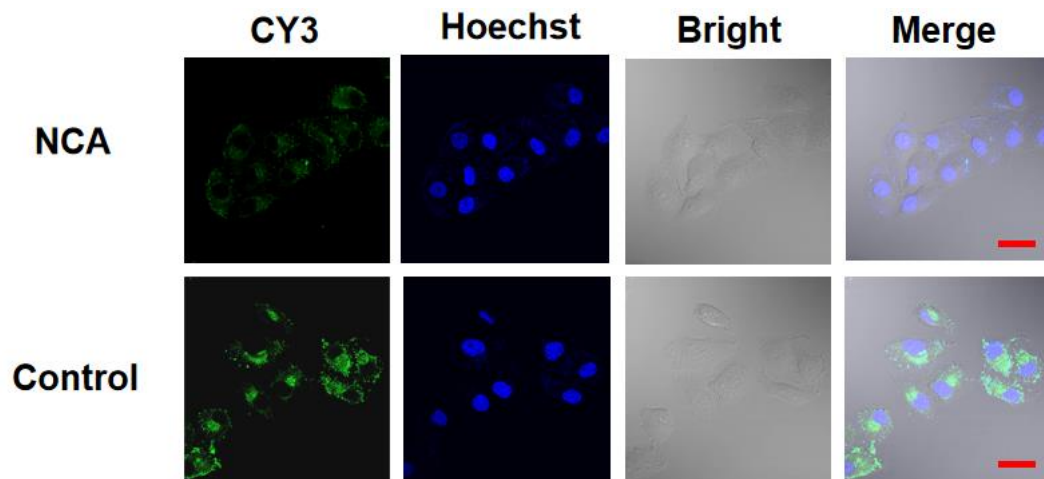


Figure S13. CLSM images of MCF-7 cells treated with 10 μ M NCA, followed by the imaging with DNA walker. Scale bar is 30 μ m.

S10. Optimization of imaging time.

We further optimized the timing for this strategy to image intracellular ATP. After the DNA walker incubated with MCF-7 cells for different durations, the intensity of the CY3 increased over time, indicating that the DNA walker system could effectively enter the cells (Figure S14). The fluorescence signal reached a plateau at about 1.5h; therefore, we chose a reaction time of 1.5h for subsequent experiments.

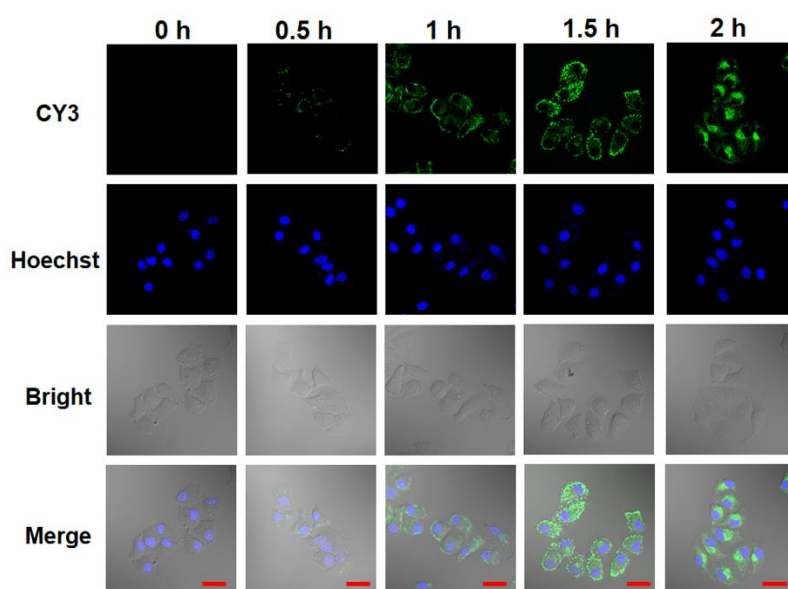


Figure S14. Confocal Microscopy Images of DNA Walker Incubated with MCF-7 Cells for Different Time. After DNA walker was incubated with MCF-7 cells for 30 min, 60 min, 90 min, and 120 min, respectively. 0 min represented the MCF-7 cells were not treated with DNA walker. Blue represents the cell nucleus stained with Hoechst 33342, while green denotes CY3 fluorescence. Scale bar is 30 μm .

S11. Monitoring changes of intracellular ATP levels.

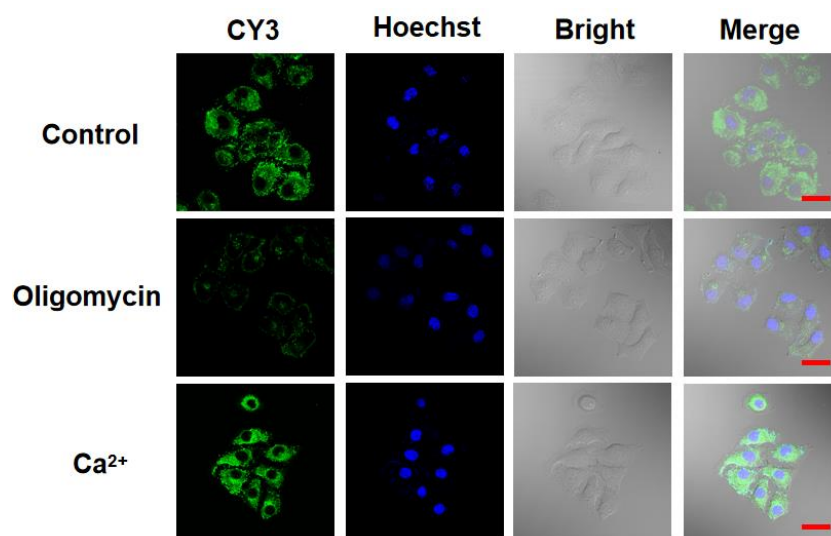


Figure S15. Monitoring intracellular ATP concentration changes by DNA walker probes. Imaging of ATP in MCF-7 cells (top) and MCF-7 cells pretreated with 10 μM oligomycin (middle) and 5 mM Ca^{2+} (bottom). Blue represents the cell nucleus stained with Hoechst 33342, while green denotes CY3 fluorescence. Scale bar is 30 μm .

S12. intracellular ATP concentration quantified by a commercial ATP assay kit.

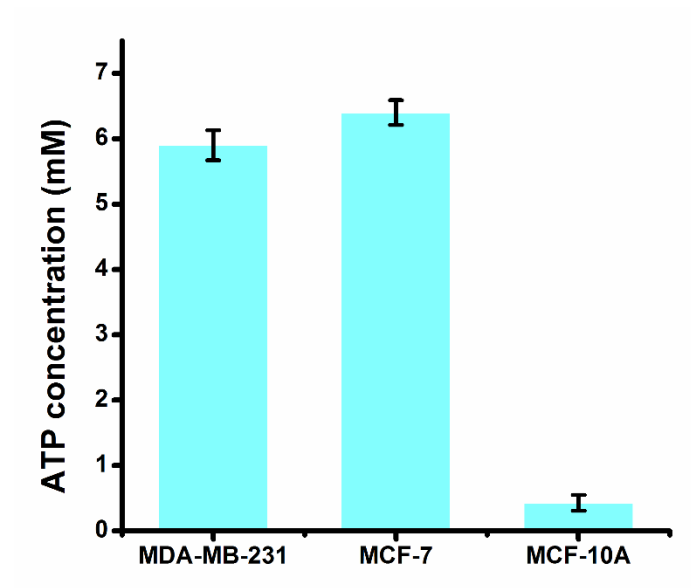


Figure S16. The intracellular ATP concentration quantified by a commercial ATP assay kit. The error bars were calculated based on the statistical results obtained from 50 cells.

S13. Comparison of this work with reported fluorescence methods for ATP detection.

Table S2. Comparison of this work with reported fluorescence methods for ATP detection.

| Analytical method | Linear range | LOD (μM) | Ref. |
|--------------------------|---------------------|---------------------------------------|-------------|
| Fluorescent | 0.01 -1 mM | 8.6 | [1] |
| Fluorescent | 0.03 - 1mM | 1.1 | [2] |
| Fluorescent | 0.125 - 2 mM | 19 | [3] |
| Fluorescent | 0.03 -2 mM | 30 | [4] |
| Fluorescent | 0 - 1.6 mM | 78 | [5] |
| Fluorescent | 0.01 - 0.3 mM | 0.3 | [6] |
| Fluorescent | 0.1 - 2 mM | 18 | [7] |
| Fluorescent | 0.01 - 10 mM | 3.43 | This work |

REFERENCES

- [1] Q.N. Li, D.X. Wang, G.M. Han, B. Liu, A.N. Tang, D.M. Kong, *Anal. Chem.*, 2023, **95**, 15725-15735.
- [2] Y. Zhou, L. Zou, G. Li, T. Shi, S. Yu, F. Wang, X. Liu, *Anal. Chem.*, 2021, **93**, 13960-13966.
- [3] Z. Liu, S. Chen, B. Liu, J. Wu, Y. Zhou, L. He, J. Ding, J. Liu, *Anal. Chem.*, 2014, **86**, 12229-35.
- [4] X.F. Zheng, R.Z. Peng, X. Jiang, Y.Y. Wang, S. Xu, G.L. Ke, T. Fu, Q.L. Liu, S.Y. Huan, X.B. Zhang, *Anal. Chem.*, 2017, **89**, 10941-10947.
- [5] S.J. Cai, J.L. Wang, J. Li, B. Zhou, C.M. He, X.X. Meng, J. Huang, K.M. Wang, *Chem. Commun.*, 2021, **57**, 6257-6260.
- [6] X. Geng, Y. Sun, Y. Guo, Y. Zhao, K. Zhang, L. Xiao, L. Qu, Z. Li, *Fluorescent Carbon Dots for in Situ Monitoring of Lysosomal ATP Levels*, *Anal. Chem.*, 2020, **92**, 7940-7946.
- [7] L.L. Li, W.Y. Lv, Y. Wang, Y.F. Li, C.M. Li, C.Z. Huang, *Anal. Chem.*, 2021, **93**, 15331-15339.